International Journal of Applied Earth Observation and Geoinformation 28 (2014) 181–192

Contents lists available at ScienceDirect

International Journal of Applied Earth Observation and Geoinformation

journal homepage: www.elsevier.com/locate/jag

Estimating soil moisture and the relationship with crop yield using surface temperature and vegetation index

M.E. Holzman[a,*], R. Rivas[a,b], M.C. Piccolo[c]

[a] Consejo Nacional de Investigaciones Científicas y Técnicas – Instituto de Hidrología de Llanuras "Dr. Eduardo J. Usunoff", República de Italia 780, B7300 Azul, Buenos Aires, Argentina
[b] Comisión de Investigaciones Científicas de la provincia de Buenos Aires, Argentina
[c] Departamento de Geografía y Turismo, Universidad Nacional del Sur, Bahía Blanca, Argentina

ARTICLE INFO

Article history:
Received 5 September 2013
Accepted 11 December 2013

Keywords:
Soil moisture
MODIS
Optical-thermal
Crop yield forecasting
Remote sensing

ABSTRACT

Soil moisture availability affects rainfed crop yield. Therefore, the development of methods for pre-harvest yield prediction is essential for the food security. A study was carried out to estimate regional crop yield using the Temperature Vegetation Dryness Index (TVDI). Triangular scatters from land surface temperature (LST) and enhanced vegetation index (EVI) space from MODIS (Moderate Resolution Imaging Spectroradiometer) were utilized to obtain TVDI and to estimate soil moisture availability. Then soybean and wheat crops yield was estimated on four agro-climatic zones of Argentine Pampas. TVDI showed a strong correlation with soil moisture measurements, with R^2 values ranged from 0.61 to 0.83 and also it was in agreement with spatial pattern of soil moisture. Moreover, results showed that TVDI data can be used effectively to predict crop yield on the Argentine Pampas. Depending on the agro-climatic zone, R^2 values ranged from 0.68 to 0.79 for soybean crop and 0.76 to 0.81 for wheat. The RMSE values were 366 and 380 kg ha^{-1} for soybean and they varied between 300 and 550 kg ha^{-1} in the case of wheat crop. When expressed as percentages of actual yield, the RMSE values ranged from 12% to 13% for soybean and 14% to 22% for wheat. The bias values indicated that the obtained models underestimated soybean and wheat yield. Accurate crop grain yield forecast using the developed regression models was achieved one to three months before harvest. In many cases the results were better than others obtained using only a vegetation index, showing the aptitude of surface temperature and vegetation index combination to reflect the crop water condition. Finally, the analysis of a wide range of soil moisture availability allowed us to develop a generalized model of crop yield and dryness index relationship which could be applicable in other regions and crops at regional scale.

1. Introduction

With the increase in global food and energy demand, the monitoring of crop yield is essential for the food security. Argentina is one of the six most important producers of wheat, maize and soybean (UNDP, 2009). However, like in several countries, the main cause of instability in crop yield is the dependency on soil moisture variability, as the crops grow without irrigation. Since these crops play a considerable role in global food security, their pre-harvest yield prediction is fundamental for supporting export-import policies.

Despite the importance of soil moisture for crop yield, reliable determination of this variable at regional scales through conventional point measurements is complex. Generally, these methods are expensive and available at a limited number of stations. Moreover, high uncertainties may exist because many factors affect the spatial variability of soil moisture (e.g. changes in topography, types of soil and depth of water table). Thus, the applicability at regional scales is limited (Crow et al., 2005; Grayson and Western, 1998). In this context, it is fundamental to develop independent methods of ancillary data for soil moisture assessment and the impact on crop yield.

In the last decades several satellite-based techniques have been developed for soil moisture sensing (Batlivala and Ulaby, 1977; Chauhan et al., 2003; Du et al., 2000; Dubois et al., 1995; Jackson et al., 1977, 1996; Moran et al., 1994; Sandholt et al., 2002; Wang and Qu, 2009). These are based on information of optical-thermal and microwave bands of the electromagnetic spectrum. Microwave sensors have the capability to monitor the surface under all-weather conditions, while optical-thermal sensors can sense only in clear skies. The main disadvantage of passive microwave sensors is the coarse spatial resolution (25–40 km), so they can be used only to estimate large-area soil moisture. This limitation has been overcome partially with active microwave sensors, which have better spatial resolution (10–30 m), although with repeat intervals

* Corresponding author. Tel.: +54 2281432666.
E-mail address: mauroh@faa.unicen.edu.ar (M.E. Holzman).

0303-2434/$ – see front matter © 2013 Elsevier B.V. All rights reserved.
http://dx.doi.org/10.1016/j.jag.2013.12.006

between 15 and 25 days (Mallick et al., 2009). On the other hand, microwave sensors can monitor only near-surface soil moisture (0–10 cm) (Eagleman and Li, 1976; Jackson et al., 1982; Shutko, 1982). This is an important variable that influences the interactions between the land surface and atmospheric process (Brubaker and Entekhabi, 1996), but it is not decisive for the process determining the crop yield, as vegetation can extract deeper soil moisture. Even though information of diverse bands of electromagnetic spectrum can be combined, efforts should be made in optical-thermal infrared bands since they have an adequate spatial and temporal resolution for monitoring soil moisture and crop condition.

In this sense, several authors have analyzed canopy water stress based only on thermal infrared band data (Boulet et al., 2007; Nemani et al., 1993; Carlson et al., 1995; Sandholt et al., 2002). A direct relationship between soil moisture and land surface temperature (LST) is not evident, as LST shows sensitivity differently for vegetation and for soil below it. However, soil moisture content is an essential factor that affects the LST (Mallick et al., 2009; Sandholt et al., 2002). These concepts were originally proposed by Jackson et al. (1977, 1981) and Jackson (1982) who defined the crop water stress index (CWSI), which is based on the difference between canopy and air temperature as a function of vapor pressure deficit. About this index, Moran (2004) has shown that it would be applicable only over full vegetated areas where sensed temperature is equal to the temperature of the vegetation.

On the other hand, different authors (e.g., Carlson et al., 1994; Goetz, 1997; Han et al., 2010; Mallick et al., 2009; Moran et al., 1994; Nemani and Running, 1997; Sandholt et al., 2002) have examined the capability of capturing information about surface water and energy availability combining satellite data of land surface temperature (LST) and vegetation indices (VI). LST and vegetation condition largely depend on water availability. Soil moisture controls the partitioning of energy between latent (evapotranspiration) and sensible heat fluxes (Monteith, 1981). The lower latent flux, the more energy available for sensible heating of the surface. In addition, plants can exert physiological control over the stomatal resistance to transpiration according to the soil moisture availability. Thus, LST increases in early stages of water stress process (Goetz, 1997). In advanced stages of water stress, root zone soil moisture is minimal and the photosynthetic systems (e.g. pigments content) are affected, decreasing the VI. Thereby, short and long-term variations of soil moisture and the impact on vegetation condition could be monitored through stress indices combining LST, visible and NIR information. One of them is the Temperature Vegetation Dryness Index (TVDI), based on a parameterization of the relationship between LST and a vegetation index (Sandholt et al., 2002), being calculated from satellite imagery without ancillary data and can be applicable over partially vegetated surfaces.

Earlier works have analyzed the relationship between TVDI and soil moisture. Sandholt et al. (2002) showed that TVDI from NOAA-AVHRR (Advanced Very High Resolution Radiometer) can reflect the spatial variation of simulated soil moisture at landscape scale in a semiarid area of Senegal. Patel et al. (2009) estimated soil moisture in a sub-humid area of India with TVDI from 8 day MODIS (Moderate Resolution Imaging Spectroradiometer) reflectance and surface temperature products. Mallick et al. (2009) estimated near-surface soil moisture (0–5 cm) in India through the soil wetness index (SWI), an index similar to TVDI. Using data from ASTER (Advanced Space borne Thermal Emission and Reflection Radiometer) for field scale and MODIS AQUA for landscape scale, they found better results at landscape scale than in field scale as ASTER fails to capture the wide range of surface soil wetness and vegetation cover required in this method. Han et al. (2010) estimated surface soil moisture in China with MODIS TERRA data products of 16-day composite NDVI and 8-day composite LST. These authors found a strong correlation between TVDI and relative soil moisture, with $R^2 = 0.76$. Chen et al. (2011) also reported a strong relationship between TVDI, rainfall data, phenological development and surface soil moisture (10–20 cm) in China. In Argentina, Holzman and Rivas (2011) reported that TVDI is suitable to reflect the spatial and temporal variability of soil moisture in Argentine Pampas at regional scale.

About crop yield estimation, plants condition and forecast yield have been extensively analyzed in many countries through the traditional Normalized Difference Vegetation Index (NDVI) (Boken and Shaykewich, 2002; Doraiswamy and Cook, 1995; Mkhabela et al., 2005, 2011; Moriondo et al., 2007; Quarmby et al., 1993). These studies are based on that photosynthetic capacity of vegetation, spectrally estimated through these indices, is directly related to crop yield. Most of these works have reported linear correlation between NDVI and crop yield. Mahey et al. (1993) reported that NDVI during maximum vegetation cover stage is linear and closely related to wheat yield. Baez-Gonzalez et al. (2002), through NOAA-AVHRR, determined that yield of maize can be estimated in Mexico 1–2 months before harvest. Also Unganai and Kogan (1998) had found that NDVI from NOAA-AVHRR correlated significantly with maize yield in Zimbabwe during the grain filling stage. Prasad et al. (2006) estimated crop yield in United States with rainfall, NDVI, surface temperature and soil moisture data and reported $R^2 = 0.78$ for corn and $R^2 = 0.86$ for soybean crops. In spite of the extensive use of NDVI, this index can saturate at Leaf Area Index values between 2 and 6 (Carlson and Ripley, 1997; Wang et al., 2005), with limitations for monitoring vigorous vegetation. Moreover, vegetation indices are conservative indicators of vegetation condition, as vegetation remains in good conditions after initial water shortages (Gillies and Carlson, 1995).

In spite of numerous works about surface soil moisture estimation through TVDI, the relationship with crop yield has yet to be examined. Therefore, the main objective of this work was to evaluate the ability to estimate regional crop yield using the TVDI. Furthermore, there were two specific objectives. The first was to validate the relationship between surface soil moisture and TVDI and finally to assess the level of precision that could be expected from this method to estimate crop yield.

2. Temperature Vegetation Dryness Index

2.1. Theory

The LST mainly depends on soil moisture and fractional vegetation cover. In bare soil and vegetated surfaces, soil moisture determines surface temperature through evaporative control, thermal inertia and the amount of energy involved in the evapotranspiration process (Mallick et al., 2009), with differences in radiative temperature between soil and canopy. Thus, combination of fractional vegetation viewed for the sensor through VI and LST allows the estimation of soil water availability from bare soil to full vegetated surfaces.

Typically, there is a strong negative relationship between LST and VI (Gillies et al., 1997). With increasing VI, the soil signal becomes increasingly masked by vegetation, with decreases in temperature. On the other hand, with high soil moisture availability LST decreases becoming similar on both bare soil and vegetation (Nemani et al., 1993). Thus, several authors (Carlson et al., 1994; Han et al., 2010; Price, 1990; Sandholt et al., 2002; Stisen et al., 2008; Wang et al., 2006) have proven that if a wide range of fractional vegetation cover and soil moisture contents are represented in the data, the scatterplot of LST and VI frequently shows a triangular shape. Some studies have interpreted this triangular space from the energy balance concept (e.g. Mallick et al., 2009), other considering different inter-related aspects (e.g. Sandholt et al., 2002).

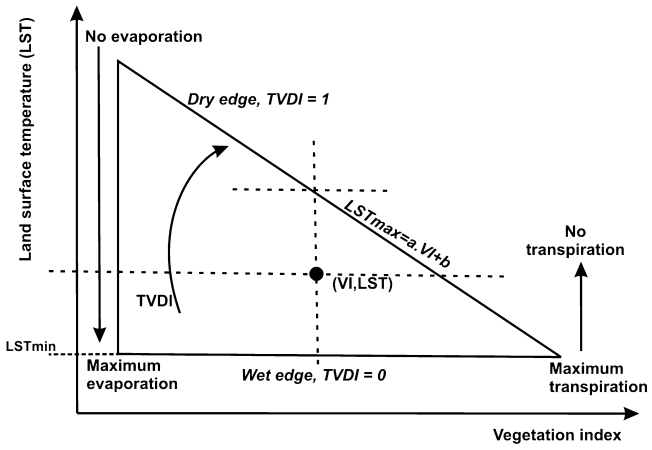

Fig. 1. Conceptual diagram of LST-vegetation index scatterplot for defining Temperature Vegetation Dryness Index (TVDI). The position of a given pixel (VI, LST) is determined mainly by soil moisture availability.
Adapted from Sandholt et al. (2002).

The conceptual LST/VI space, with LST plotted as a function of VI, is shown in Fig. 1. In the triangle, different edges can be defined representing extreme conditions of soil moisture and evapotranspiration. The dry edge represents limiting conditions of soil moisture or evapotranspiration for different VI classes. The group of points closest to the dry edge reflects very stressed surfaces, with low soil moisture in the root zone. In these points, stomatal closure for vegetated areas is a key factor, controlled by the limited moisture availability. As green vegetation increases along *x*-axis, maximum LST (LST_{max}) decreases. In this way, negative relation for dry conditions is defined by the dry edge, which reflects the limit of LST for a given value of VI. On the other hand, the base of triangle or wet edge consists of a group of points that describe a horizontal line (LST_{min}), indicating maximum soil wetness condition and potential evapotranspiration. The left edge represents bare soil, ranging from dry to wet (maximum LST to minimum LST, respectively). Thus, the location of a point in the LST/VI space is influenced mainly by soil moisture availability.

In the triangular space, to obtain information on the surface soil moisture content, the TVDI was defined (Sandholt et al., 2002):

$$\mathrm{TVDI} = \frac{\mathrm{LST} - \mathrm{LST}_{\min}}{\mathrm{LST}_{\max} - \mathrm{LST}_{\min}} \quad (1)$$

where LST is the observed surface temperature (K) at a given pixel, LST_{min} is the minimum temperature in the triangle, defining the wet edge, $LST_{max} = aVI + b$ is the maximum temperature for a given value of VI, *a* and *b* are surface parameters of the image defining the dry edge, modeled as a linear fit to the data (Fig. 1). The value of TVDI is 1 along the dry edge, indicating limited soil moisture availability and its value is 0 along the wet edge, showing unlimited water access and maximum evapotranspiration.

About the dry edge, Stisen et al. (2008) explained the difference between the theoretical and observed edges. The true dry edge represents zero surface soil moisture and zero evapotranspiration, with LST reaching a physical maximum when no evaporative cooling and complete stomatal closure occur (Moran et al., 1994). The dry edge observed in remote sensing data is defined by lower LST than the theoretical dry edge, as in reality zero evapotranspiration rarely occurs for dense vegetation. Frequently, even in semi-arid environments, vegetation can extract soil water from the root zone. In that way, the decoupling between near-surface and root zone soil moisture in vegetated pixels could allow the monitoring of deep soil moisture through LST/VI combination.

2.2. Assumptions and sources of error

It should be noted that, although the TVDI is easily obtained, a suitable estimation of the index depends on a proper definition of *a*, *b* parameters and the wet edge. These parameters should be estimated on the basis of pixels from a study area with regular atmospheric forcing and heterogeneous enough to represent the entire range of surface soil wetness, from wet to dry, and from bare soil to fully vegetated areas. Mallick et al. (2009) and Sandholt et al. (2002) have reported a number of possible error sources in operational soil wetness estimation from satellite data:

(i) View angle effects on LST and VI.
(ii) The triangle may not be correctly determined if the area of interest does not include a full range of variability in land surface conditions (e.g. dry and saturated bare soil, water stressed and well watered vegetation).
(iii) Variations in net radiation associated with cloud shadows.
(iv) Errors in LST and VI estimated from satellite data due to unknown and varying land surface emissivity and atmospheric effects.
(v) The influence of soil moisture in deeper layer on top surface soil layer (Capehart and Carlson, 1997).
(vi) Dependence of LST and VI on surface type, due to differences in aerodynamic resistance (Friedl and Davis, 1994; Lambin and Ehrlich, 1995).

These error sources should be considered using atmospherically corrected images and they could be assessed comparing estimates and measurements of different physical variables (i.e. soil moisture content) (Mallick et al., 2009).

3. Description of study area

The Argentine Pampas is a wide plain of 50 million hectares suitable for cropping and it is the most productive rainfed region of Argentina. In general, the climate is humid temperate. The rainfall regime varies in space and time, determining occasional extreme conditions of droughts and floods over wide areas (Viglizzo et al., 1997). Four agro-climatic zones with different soil and climatic characteristics were selected for crop yield estimation and validation: Sandy Pampas, Endorreic Pampas, Northern hills, Semi-arid Plains (see Table 1 and Fig. 2 for location, and agro-climatic characteristics). The study area represents a wide variety of soil types. In general, Endorreic Pampas and Northern hills show the best soil conditions for cropping, as the high water retention capacity of soils. Moreover, organic matter and the granular structure of soils decrease from the humid (Endorreic Pampas and Northern hills) to semi-arid and sandy zones. Ratio (R/PE) of annual rainfall (R) and potential evapotranspiration (PE) varies between 0.80 (Semi-arid Plains) and 1.43 (Northern hills). Thereby, the humid zones show sufficient rainfall to supply crop water consumption, with frequent soil water excess in Northern hills. In Semi-arid Plains water deficits during the summer (January and February) are usual, with limiting conditions for several crops.

About the land use, during the last decades Argentine Pampas has exhibited an increasing allocation of land to agricultural activities and an intensification of farming on existing lands (Viglizzo and Frank, 2006). Thus, nowadays the agriculture is based on a few crops, which the most extended and representative over the analyzed agro-climatic zones are soybean as summer crop and wheat as winter crops.

Table 1
Agro-climatic characteristics of the study area.

Analyzed agro-climatic zones	Central coordinates		Main crop (% covered area)	Soil type	R/PE
	Longitude	Latitude			
Sandy Pampas	61°40′ W	35°15′ S	Soybean (25%)	Udipsamment	1.00
Endorreic Pampas	63°22′ W	33°55′ S	Soybean (26%)	Hapludoll and Haplustol	1.05
Northern hills	59°05′ W	37°17′ S	Wheat (30%)	Typic Argiudoll	1.43
Semi-arid Plains	63°38′ W	36°48′ S	Wheat (12%)	Haplustoll	0.80

R/PE = Annual rainfall (mm)/Annual pan evaporation (mm).

4. Materials and methods

4.1. Satellite data

MODIS AQUA 8-day composite surface temperature, level-3, version-5, 1 km (MYD11A25) and 16-day composite vegetation index level-3, version-5, 1 km (MYD13A25) were used to calculate the TVDI. Wang et al. (2007) found that the lag time for VI to respond to soil moisture change is about 5 days at the semi-arid sites and 10 days at the humid sites. Due to the fact that the study area is a semiarid and sub-humid zone and MODIS VI product is 16-days composite, the effects of soil moisture on vegetation should be reflected in the composite VI. The theory of these indices is based on properties of vegetation to reflect the incident solar radiation differently in the red and near-infrared spectral wavebands. The chlorophyll pigment present in leaves causes lower spectral reflectance in red band than in infrared band, being this relationship reverse in case of unhealthy vegetation, e.g. under water stress (Kogan, 1994). Among these indices, the most extended is the NDVI, however different authors (Huete and Liu, 1994; Kaufman and Tanré, 1992) have reported that atmospheric aerosols dispersion reduces the difference between red and IR reflectances. Huete and Liu (1994) found that NDVI decreases with the increase in atmospheric aerosol contents as well as background influence. Therefore, the traditional TVDI method proposed by Sandholt et al. (2002) using NDVI was modified in this work. NDVI was replaced by the EVI, which has been developed to correct the canopy background and atmospheric influences with improved sensitivity into high biomass regions (Liu and Huete, 1995):

$$\mathrm{EVI} = G\frac{(\rho_{\mathrm{NIR}} - \rho_{\mathrm{red}})}{(\mathrm{NIR} + C_1\rho_{\mathrm{red}} - C_2\rho_{\mathrm{blue}} + L)} \quad (2)$$

were ρ_{NIR} and ρ_{red} represent the reflectance of the near infrared and red bands, respectively; G is a Gain factor; C_1 and C_2 are the coefficients of the aerosol resistance term, which uses the blue band to correct for aerosol influences in the red band; and L operates as a soil soil-adjustment factor. $L = 1$, $C_1 = 6$, $C_2 = 7.5$ and $G = 2.5$. EVI has values between −1 and +1. Huete et al. (2011) have reported that the MODIS EVI values vary from 0.07 for hyperarid deserts to 0.7 to dense forests at 1 km resolution. Stressed or sparse vegetation has reduced positive values (Basnyat et al., 2004).

The satellite data were acquired from NASA's Earth Observing System Data and Information System (http://reverb.echo.nasa.gov/reverb) in Sinusoidal projection and were processed with ENVI software and reprojected using MODIS conversion toolkit to Geographic Lat/Lon coordinates, Datum WGS-84. A subset of the study area was defined (31°46′ 13.80″ S–68°13′ 41.79″ W and 39°55′ 48.95″ S–51°30′ 54.01″ W). Several authors (Benedetti and Rossini, 1993; Hochheim and Barber, 1998; Mkhabela et al., 2005) have shown that using average VI of 3–4 weeks increased the coefficient of determination and stabilized the regression models, taking into account only vegetation responses and the cumulative effect of photosynthesis. Thus, LST and EVI images of that subset were averaged to obtain monthly TVDI images. Over semi-arid areas there is a high probability of TVDI underestimation, as pixels with minimum LST are limited. On the other hand, dry edge definition is difficult over humid zones. Thus, dry and wet edges were estimated based on LST/EVI scatter plot of semiarid and humid areas (390 km × 390 km each of them), respectively. The former edges were obtained using the least square method, significance level of 5%. The latter ones were calculated averaging the pixels with minimum LST in the LST/EVI scatterplots. To obtain comparable TVDI values among different periods, dry (maximum slope and intercept) and wet (minimum $\mathrm{LST}_{\mathrm{min}}$) extreme edges were defined

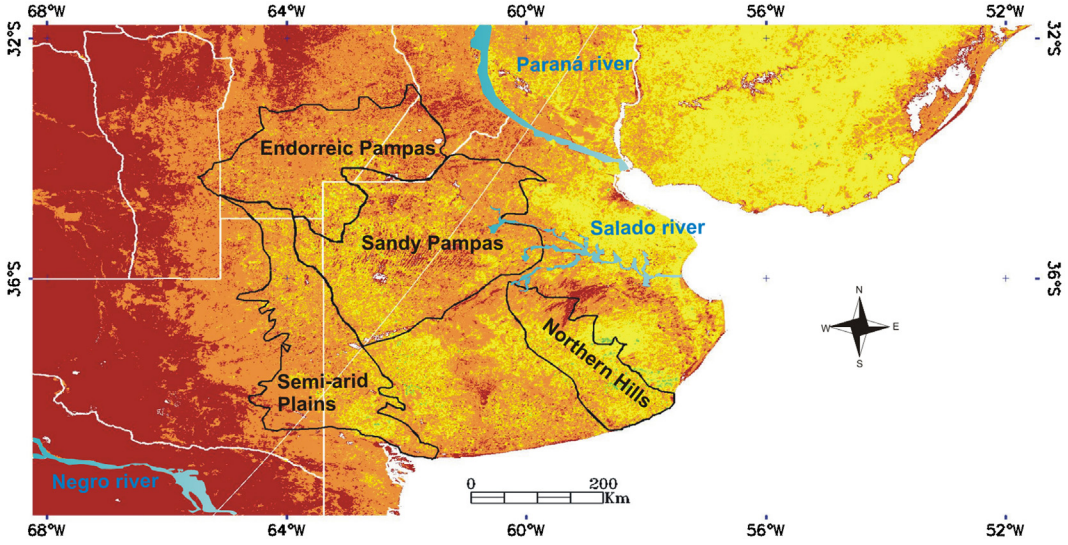

Fig. 2. Locations of the analyzed agro-climatic zones of Argentine Pampas.

(Holzman et al., 2012). Finally, monthly TVDI images were computed with theses edges.

The TVDI data included severe drought (2007–2008), normal (2009–2010, 2010–2011) and high (2002–2003) soil moisture conditions, allowing us to test the methodology over a wide range of crop conditions. Critical growth stage (flowering and grain filling) was considered to analyze TVDI/crop yield relationship, as it is the most decisive for most crops yield. Water stress during this stage would result in reduced grain yield. According to Oficina de Riesgo Agropecuario-Ministerio de Agricultura, Ganadería y Pesca de Argentina (ORA-MAGyP, http://www.ora.gov.ar), for soybean this stage includes January and February in Sandy and Endorreic Pampas. For wheat, in Northern hills and Semi-arid Plains November-December and October-November were considered. Inside these zones, crop cover regions of interest that included only cultivated areas were defined for each county. The objective was to eliminate the effect of uncultivated areas on the TVDI signal.

4.2. In situ measurements

Although different authors (Han et al., 2010; Mallick et al., 2009; Sandholt et al., 2002) have shown TVDI/surface soil moisture relationship, this was daily and monthly validated for our study area. Soil moisture measurements were carried out monthly in Campus Tandil station (Northern hills, 37°19′ S, 59°05′ W) and daily in La Ydalina station (Sandy Pampas, 35°09′ S, 61°07′ W). The periods included November 2009 to March 2010 and November 2010 to February 2011 on Campus Tandil station and January–February 2012 on the second station. On Campus Tandil, calibrated EC-10 H_2O (Decagon Devices, Inc.) and EC-20 H_2O single panel soil moisture probes were used for this purpose. The EC-10 H_2O and EC-20 H_2O measure the integrated dielectric constant (mV) at 10 cm and 20 cm, respectively, which is directly related to the volumetric water content (VWC). The accuracy of these probes has been verified in Tandil station with field data and is higher than 97% (Carmona et al., 2011). To convert mV output of probes (at 10 cm and 20 cm depth) to VWC ($m^3\ m^{-3}$) the Eqs. (3) and (4) provided by manufacturer were used:

$$VWC_{EC-10H_2O} = (0.00093\,mV - 0.376) \quad (3)$$

$$VWC_{EC-20H_2O} = (0.00069\,mV - 0.29) \quad (4)$$

Monthly TVDI of a homogeneous crop patch of 3 km × 3 km were compared with soil moisture measurements located at the center of that patch. On Sandy Pampas (La Ydalina station), soil moisture condition was measured daily at 60 cm depth with a tensiometer incorporated into a Vantage Pro2 station (Davis Instruments). Tension values can vary from 0 to 200 centibars indicating maximum and minimum soil moisture availability, respectively. Then 25 measurements located in the center of a patch of 3 km × 3 km were compared with daily TVDI under clear sky conditions.

4.3. Crop yield data

Statistics Argentina collects comprehensive data on the entire cultivated area, including yield of the main crops over Argentina. Official statistics of soybean and wheat yield ($kg\ ha^{-1}$) during the study period were obtained at county level from Statistics Argentina (Statistics Argentina, 2012). Over these periods the evaluated crops were the most spatially extended in the analyzed agro-climatic zones. Regression analysis was done separately for each crop in each zone. Yield data (dependent variable) were correlated with averaged TVDI (independent variable) of the cultivated areas in the following counties: Carlos Casares, Carlos Tejedor, Pellegrini (Sandy Pampas), Gral. Roca, Gral. Villegas (Endorreic Pampas), Tandil, Azul (Northern hills), Trenel and Capital (Semi-arid Plains) (see surfaces in Table 2).

Table 2
Surface counties considered for TVDI/crop yield relationship (YR) and validation (YV).

Agro-climatic zones	County	Surface (km^2)
Sandy Pampas	Carlos Tejedor (YR)	5539
	Carlos Casares (YR)	3561
	Pellegrini (YR)	2660
	General Viamonte (YV)	3020
	Bolívar (YV)	7022
	Tres Lomas (YV)	1782
Endorreic Pampas	General Roca (YR)	15,288
	General Villegas (YR)	7606
	General López (YV)	15,743
	Roque Sáenz Peña (YV)	10,287
Northern hills	Tandil (YR)	3504
	Azul (YR)	1947
	Olavarría (YV)	3727
	Benito Juárez (YV)	2785
	Balcarce (YV)	2847
Semi-arid Plains	Capital (YR-YV)	2500
	Trenel (YR)	1989
	Realicó (YV)	2643

It should be noted that soil moisture availability during initial growth stage determines plants density while such condition on critical growth stage defines crop yield (Mkhabela et al., 2005). In addition, different authors (Mkhabela and Mkhabela, 2000; Rasmussen, 1992; Unganai and Kogan, 1998) have reported that cumulative NDVI of critical growth stage correlated better with crop yield than when the whole growing period is included. Crop yield was correlated with cumulative TVDI of critical growth stage. To test the robustness and the ability of the generated regression models to forecast crops grain yield, estimated and observed yield data were compared on counties or dates previously not considered: Gral. Viamonte, Tres Lomas, Bolivar (Sandy Pampas), Gral. López, Roque Saenz Peña, Gral. Roca (Endorreic Pampas), Realicó, Capital (Semi-arid Plains) (Table 2). The performance of the models was assessed using root mean square error (RMSE), bias and index of agreement d (Willmott, 1981):

$$RMSE = \sqrt{\frac{\sum_{i=1}^{N}(O_i - E_i)^2}{N}} \quad (5)$$

$$Bias = \frac{\sum_{i=1}^{N}(O_i - E_i)^2}{N} \quad (6)$$

$$d = 1 - \frac{\sum_{i=1}^{N}(O_i - E_i)^2}{\sum_{i=1}^{N}(|E_i - \bar{O}| + |O_i - \bar{O}|)^2} \quad (7)$$

where N is the number of observations, O_i and E_i are the observed and estimated values, respectively. The bias is an indicator of overestimation (−) and underestimation (+). The d index values vary between 0 and 1 indicating low and high relationship between estimated and observed values, respectively. The model is perfect when $d = 1$ and bias = RMSE = 0.

5. Results and discussion

5.1. LST-EVI scatterplots

Monthly dry and wet edges were determined from LST-EVI scatterplots to obtain TVDI images and the relationship with crop yield over the 4 agro-climatic zones of the study area. An adequate definition of monthly dry and wet edges was achieved through scatterplots of semi-arid and humid areas, respectively. Table 3 shows

Table 3
Monthly and extreme wet edges of study period.

Month	Wet edge (K)	Month	Wet edge (K)	Month	Wet edge (K)	Month	Wet edge (K)
2002–Oct.	295.3	2007-Oct.	295.4	2009-Oct.	**293.9**	2010-Oct.	294.8
2002–Nov.	**296.6**	2007-Nov.	298.5	2009-Nov.	297.0	2010-Nov.	299.3
2002–Dec.	298.5	2007-Dec.	303.5	2009-Dec.	**297.6**	2010-Dec.	303.2
2003–Jan.	**300.8**	2008-Jan.	301.5	2010-Jan.	301.9	2011-Jan.	302.2
2003–Feb.	299.0	2008-Feb.	300.9	2010-Feb.	**298.5**	2011-Feb.	299.8

monthly and extreme (shown in bold) wet edges, which were used to calculate TVDI images. The values of wet edges varied between 293.9 K (October 2009) and 303.5 (December 2007), consistent with the increase of LST and incoming radiation during the main summer months.

The 20 obtained dry edges from October to February are shown in Fig. 3. The large swath width (2330 km) and moderate resolution (1 km) of MODIS AQUA sensor captured the soil moisture and vegetation cover spatial heterogeneity required by TVDI method. A wide range of EVI and LST data was visible for all scatterplots, with increasing values from October to February and reaching maximum EVI of 0.8 in most cases and LST of 325 K (i.e. January 2008). This general trend is consistent with dominant crops (soybean) summer growth that rich maximum vegetation covers in January and February and with the increasing incoming solar radiation.

On the other hand, different growth characteristics with respect to water availability for crops can be inferred from dry edge parameters. There were months characterized by a narrow dynamic range of LST: October 2002 (295–307 K), October (297.5–308.5 K) and November 2007 (304–316 K) and October 2010 (305–315 K). This is visible in a relatively flat dry edge slope and low intercept, which indicate high soil moisture availability, elevated evapotranspiration and consequently the relative homogeneity of LST. In addition, there were months with the opposite situation indicating low soil moisture availability, for example: January 2008 (303–325 K), February 2008 (301–322 K), January 2010 (303–325 K). The minimum (309.4 K) and maximum (335.5 K) intercept were observed in October 2002 and December 2010, indicating high and low soil moisture availability, respectively (Fig. 3). Different authors (Chen et al., 2011; Gillies et al., 1997; Goward et al., 2002; Sandholt et al., 2002) have reported low TVDI values after rainfall events. It should be noted that, even though each analyzed period can be characterized by general wetness condition, the parameters of each month vary according to the rainfall.

On the scatterplots of analyzed months strong linear correlation was obtained with R^2 between 0.87 and 0.99, indicating that dry edges are adequately represented by linear equation (Fig. 3). These results are in agreement with previous works using images of ≈1 km spatial resolution (Chen et al., 2011; Sandholt et al., 2002; Tang et al., 2010) that shown $R^2 > 0.80$.

5.2. Spatial variation of TVDI

With the extreme dry and wet edges monthly TVDI images were obtained. In the TVDI maps (Fig. 4), the spatial distribution of the dryness index for two periods with opposed wetness condition is shown: wet (2002–2003) and dry (2007–2008). A large spatial and temporal variability of moisture availability is evident. Usually, dry and very dry conditions (TVDI > 0.6) are located in arid and semi-arid areas on the west of the region, opposed to humid ones on the east where the oceanic influence is noticeable. Moist areas around the rivers have low dryness index values (i.e. Negro river), similar to surfaces with vigorous vegetation cover where the evapotranspiration is high. The TVDI also reflects depressions in the landscape showing a low index corresponding to moist surface conditions and shallow water table, e.g., the Salado river basin on the east of the region or Paraná basin on the north side (Fig. 4, December 2002 to February 2003).

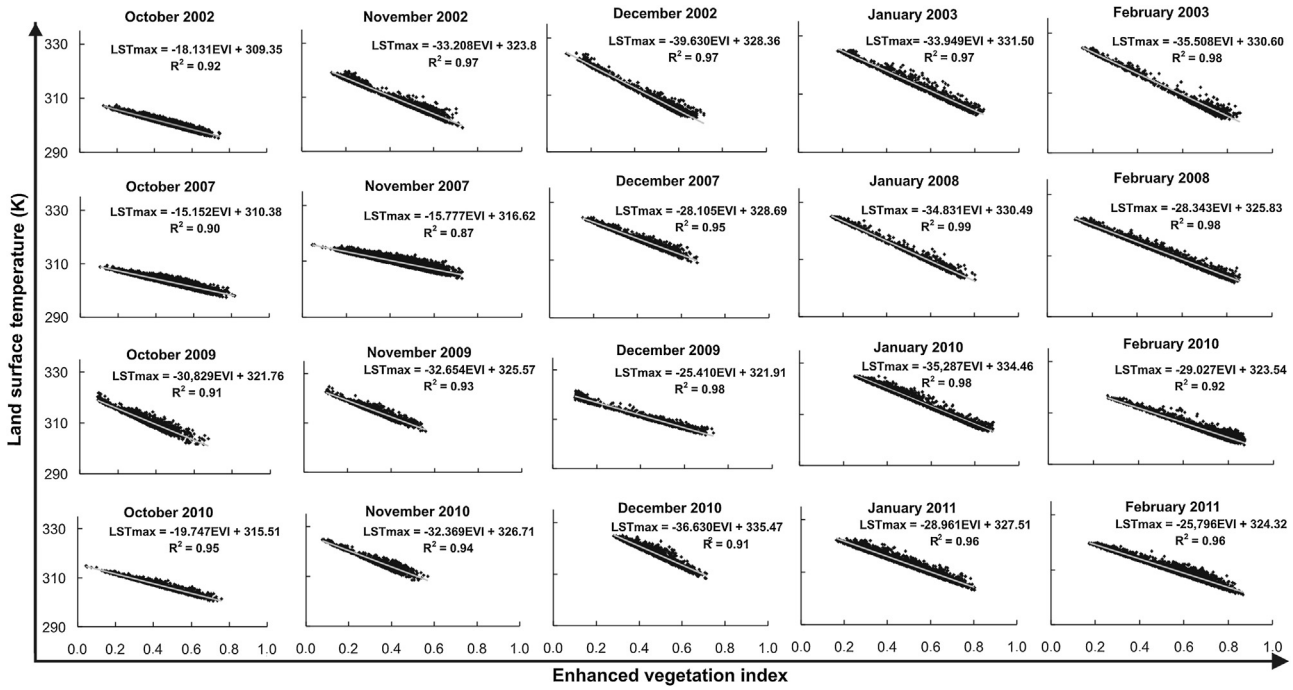

Fig. 3. Dry edges from MODIS AQUA over the four study periods.

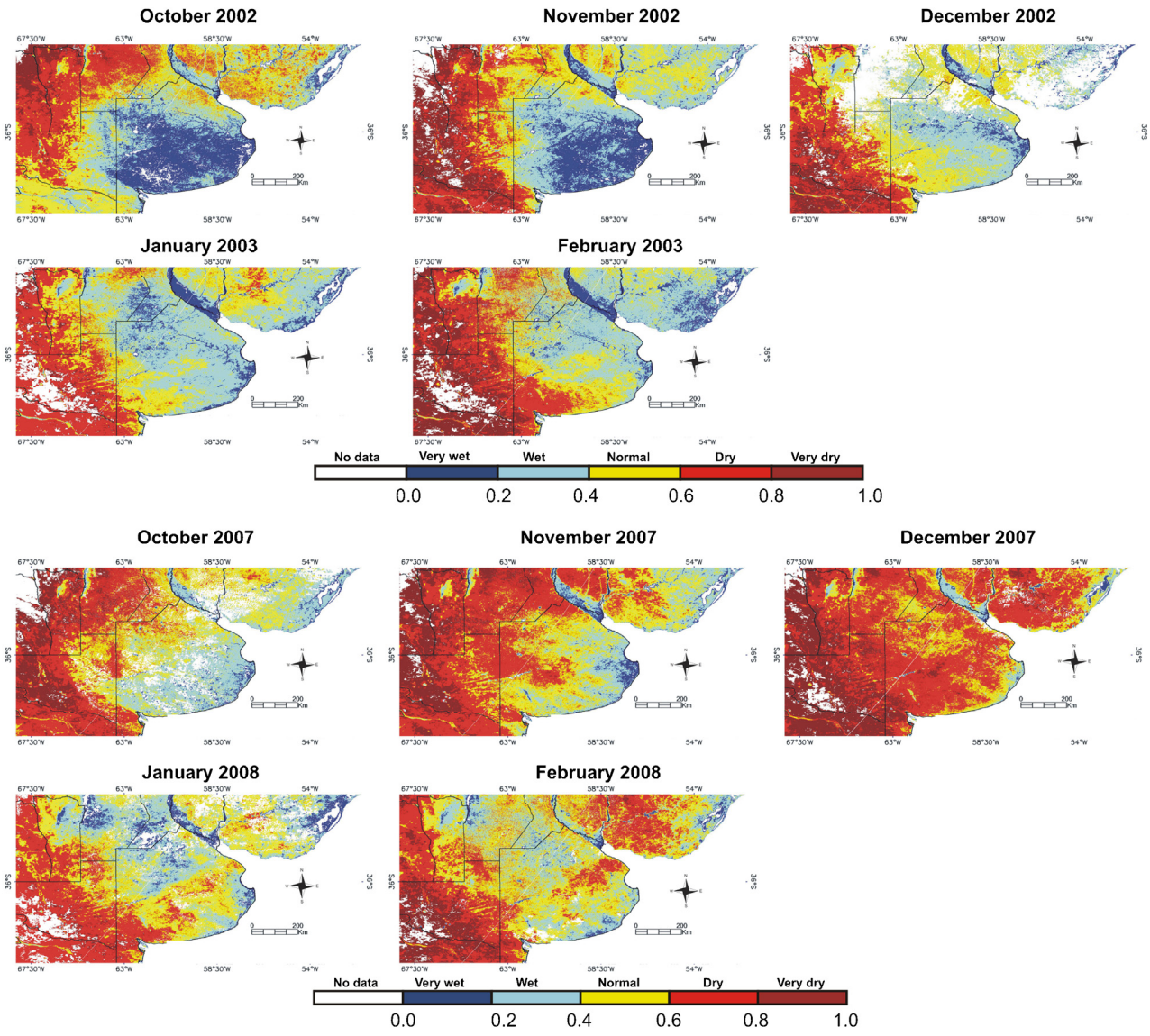

Fig. 4. Maps of TVDI for two analyzed periods with contrasting wetness condition: wet (2002–2003) and dry (2007–2008). There were masked areas due to clouds or lakes.

Regarding the temporal variation, generally dry conditions extend eastward from November to February in agreement with increasing atmospheric evaporative demand, with irregular spatial pattern according to the rainfall distribution (Fig. 4). 2002–2003 can be defined as a humid period, with excessive moisture in October and November. On the other hand, 2007–2008 is characterized with widespread dry and very dry conditions, covering large surfaces of the most productive central and eastern areas. In general, December, January and February showed the lowest soil moisture availability, with critical situation in December 2007 affecting most of Sandy Pampas, Endorreic Pampas and Northern hills (Fig. 4). It should be noted that these three months are especially important for summer crops (i.e. soybean) as they cover the critical growth stage. Thus, intense water deficits during this period are frequently regional production constraints. Particularly, the rainfed soybean crop is the dominant in most of the study area during January and February, usually growing during these months with residual soil moisture. Consequently, soybean crop yield largely depends on spatial variability of soil wetness during these determining months.

5.3. Comparison to soil moisture measurements

Although previous works have analyzed the TVDI/soil moisture relationship, to prove the effectiveness of the methodology in the study area, TVDI was compared with monthly (Fig. 5) and daily (Fig. 6) in situ soil moisture measurements. Monthly soil moisture data plotted as a function of TVDI show that higher values correspond to lower TVDI. Linear relationship was found with R^2 values ranging from 0.61 to 0.83 (Fig. 5). Regarding daily soil moisture data, it should be noted that the values are expressed in centibars as the water retention curve of soils in the station still are being calculated. However, the relationship between TVDI and these data are evident, with R^2 value of 0.75 (Fig. 6). Earlier studies have compared TVDI and direct estimation of soil moisture content. In China, Wang et al. (2004) found significant negative correlation (R^2 = 0.35–0.68) between TVDI from NOAA-AVHRR and surface soil moisture. Han et al. (2010) with MODIS TERRA images found in China linear correlation (R^2 = 0.76) at monthly scale. In India, with MODIS AQUA at landscape scale Mallick et al. (2009) reported R^2 = 0.88 between SWI (similar to TVDI), and near-surface soil moisture (0–5 cm). These

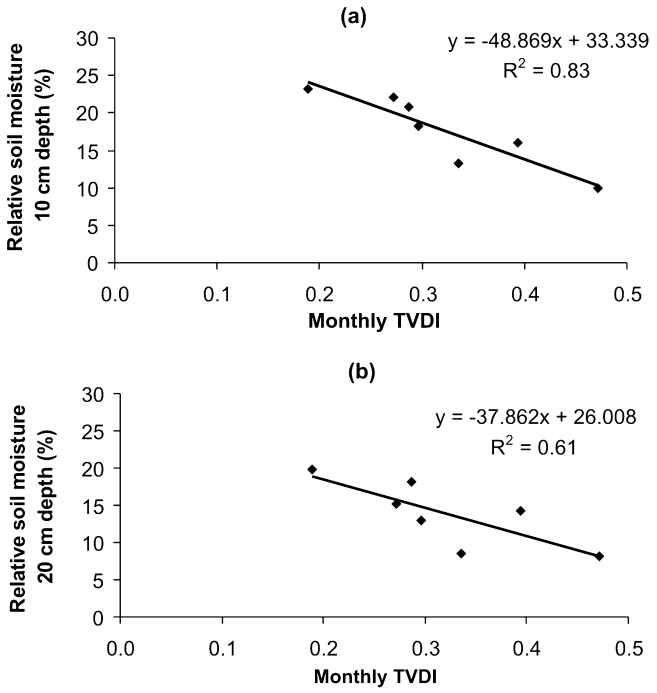

Fig. 5. Scatterplots of corresponding monthly TVDI and soil moisture measurements for Campus Tandil (Northern hills).

results demonstrate the ability of the TVDI to reflect spatial and temporal variation of soil moisture content.

5.4. Crop yield and TVDI

Fig. 7 shows the relationship between cumulative TVDI over critical growth stage, soybean and wheat crop yield in the four analyzed agro-climatic zones. Regarding to soybean, in Sandy and Endorreic Pampas critical growth stage includes January and February. The wide range of the cumulative dryness index (TVDI 0.54–1.27) and crop yield (1712 kg ha^{-1}–3355 kg ha^{-1}) allowed us to evaluate the relationship over different wetness condition. In both zones the TVDI is highly correlated with grain yield, while the highest correlation (R^2 = 0.79) is observed in Endorreic Pampas. This indicates that the developed models explained up to 79% of the variability of soybean crop yield. For both cases the relationship was best described by a linear function, indicating that yield decreased with increased water stress (Fig. 7a and b). These results are in agreement with previous studies which have reported high correlation between dryness indices and soybean grain yield. Rhee et al. (2010), combining LST and NDVI from MODIS sensor and precipitation estimates from Tropical Rainfall Measuring Mission (TRMM) found

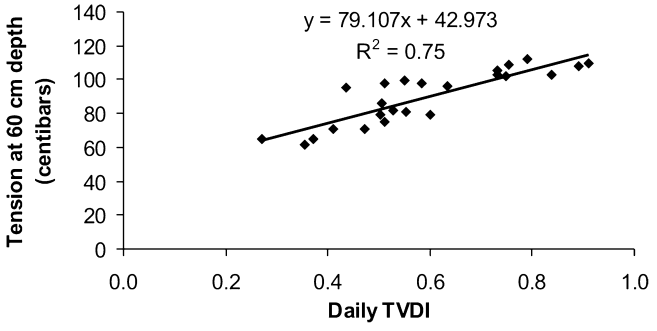

Fig. 6. Scatterplots of corresponding daily TVDI and tension measurements for La Ydalina (Sandy Pampas) at 60 cm depth.

linear trend and high correlation coefficient values (r = 0.78–0.92) for soybean in arid and humid regions of USA. O'Shaughnessy et al. (2011) reported R^2 values ranged from 0.83 to 0.88 between soybean yield and CWSI in irrigated areas at field scale. On the other hand, earlier works have shown high linear correlation between NDVI and crop yield (Marti et al., 2007; Mkhabela et al., 2005; Unganai and Kogan, 1998). Ma et al. (2001) found R^2 values ranged from 0.44 to 0.80 between soybean yield and NDVI in Canada, at field scale.

It should be noted there are slight differences between the obtained adjustments (Fig. 7a and b). The slope was higher in Sandy Pampas (2036 kg ha^{-1}) than Endorreic Pampas (1820 kg ha^{-1}). The lower slope in the second most likely indicates that the soils have higher water retention capacity, therefore soybean yield and water conditions are more stable in this zone. This is also noticeable on dynamic ranges of cumulative TVDI: 0.54–1.27 for Sandy Pampas and 0.55–1.16 for Endorreic Pampas.

Regarding wheat crop, in Semi-arid Plains and Northern hills there are differences in critical growth stage (Fig. 7c and d). In Semi-arid Plains this stage comes earlier due to higher air and soil temperature, reflected also in higher TVDI values. In Northern hills it comes one month later. In both cases the TVDI is highly correlated with grain yield with the highest correlation (R^2 = 0.81) in Northern hills. The lower correlation in Semi-arid Plains is probably due to the smaller fraction of wheat crop over the total area than in Northern hills. Therefore, the TVDI is influenced by other crops grown in the analyzed areas. Future studies at finer resolutions (i.e. field scale) could improve crop yield prediction models by developing techniques to discriminate crop types. However, our method means an important advance in crop yield estimation at regional scale in large areas with few crops or sparsely monitored areas. Moreover, our results are similar to those reported by Bhattacharya et al. (2011) who estimated wheat yield in semiarid regions of India through water and radiation use efficiency with MODIS AQUA images. They found R^2 values ranged from 0.80 to 0.94.

In general the results obtained for wheat crop were better than those shown in other studies based only on vegetation indices (Basnyat et al., 2004; Mkhabela et al., 2005; Moriondo et al., 2007; Wall et al., 2008) and VI/rainfall data combination (Balaghi et al., 2008), which explained up to 68% of the yield variability with errors ranged from 80 to 762 kg ha^{-1}. Vicente-Serrano et al. (2006) combining NDVI-AVHRR and drought indices reported R^2 = 0.88. Recently, Mkhabela et al. (2011) with MODIS-NDVI found R^2 = 0.47 and 0.80 in a sub-humid and semi-arid zones of the Canadian Prairies, respectively.

Regarding the regression model, the TVDI-wheat yield relationship was best described by a quadratic function, indicating that yield decreased not only with increasing water stress but also with excess. For example, in Northern hills maximum wheat yield (4950 and 5100 kg ha^{-1}) was observed in the normal period 2010/2011, while minimum yield (2300 and 1810 kg ha^{-1}) was registered in humid (2002/2003) and dry (2007/2008) periods, respectively. In the case of wheat, the evident water excess effect could be due to lower evaporative demand during winter and spring than in the case of soybean crop, which would explain the quadratic adjustments (Fig. 7c and d). Previously in irrigated maize crops of Turkey, Irmak et al. (2000) also observed decreasing yield exceeding a humid threshold of the CWSI. In addition, the differences between our regression models for both crops are in agreement with previous works that related stress indices and NDVI with crop yield. The reported results about different crops (Benedetti and Rossini, 1993; Holzapfel et al., 2009; Ma et al., 2001; Mkhabela and Mkhabela, 2000; Mkhabela et al., 2011; Quarmby et al., 1993) show that the contrasting adjustments depend on many factors including crop characteristics, soil type and several environmental parameters.

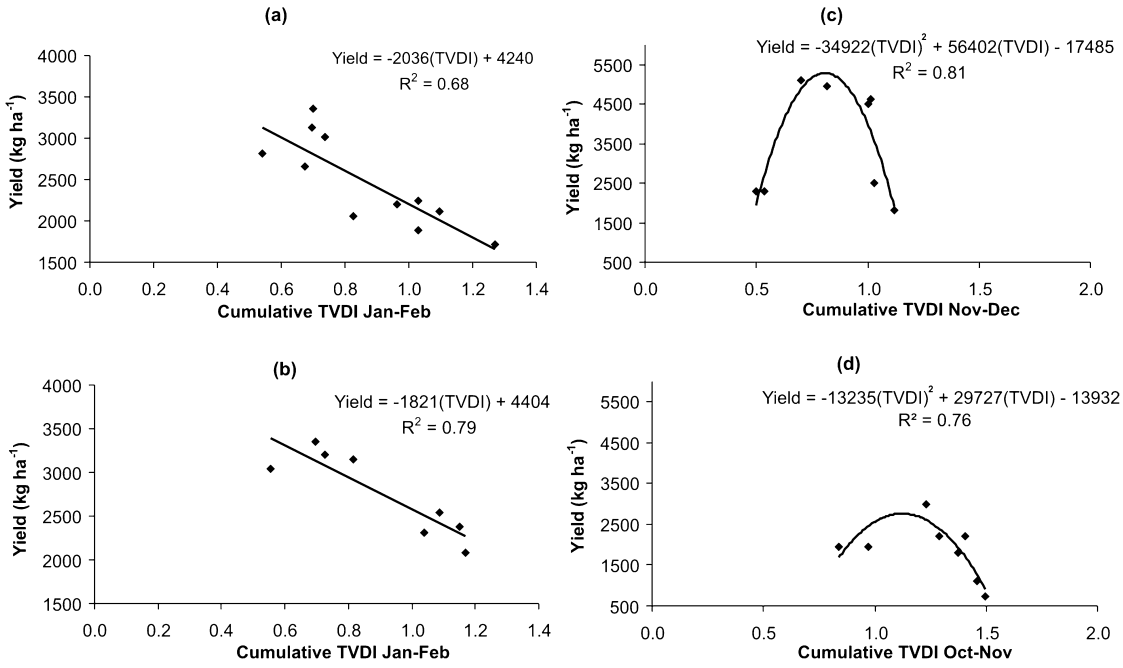

Fig. 7. Relationship between crop yield and cumulative TVDI of critical growth stage: (a) soybean in Sandy Pampas, (b) soybean in Endorreic Pampas, (c) wheat in Northern hills and (d) wheat in Semi-arid Plains.

For wheat yield some differences between the adjustments are evident in both analyzed zones (Fig. 7c and d). In Northern hills (Fig. 7c) the high production capacity explains the raised wheat yield, while different environment conditions like soil nutrients and organic matter are limiting factors in Semi-arid Plains (Fig. 7d). Finally, in Northern hills decreasing yield is more evident due to intense water excess, with contributing variables like soils with low water permeability and the more likely root zone saturation.

A comparison between satellite-derived and official statistics of soybean and wheat yield was performed to assess if satellite imagery could be successfully used to crop yield estimation (Table 4). With regard to soybean yield, for both agro-climatic zones the parameters of validation showed that the developed models predict well the yield, with RMSE values of 366 (12% of average yield) and 376 kg ha^{-1} (13% of average yield) and a slight underestimation of 169 and 216 kg ha^{-1} in Endorreic and Sandy Pampas, respectively. In both agro-climatic zones *d* index showed high relationship between estimated and observed values. Similar results were reported by Prasad et al. (2006), which using diverse data (NDVI-AVHRR, soil moisture, surface temperature, rainfall) in US found errors of 11%. About forecasting yield, our results show that TVDI from MODIS was an appropriate tool for early prediction of soybean crop yield with 2–3 months before harvest.

The results of wheat validation obtained in Northern hills and Semi-arid Plains showed a good performance of the developed models (Table 4). The results were similar to the previous ones obtained with more complex methods. Bhattacharya et al. (2011), in semiarid regions of India analyzed water and radiation use efficiency with MODIS AQUA images. These authors reported a minimum RMSE value of 337 kg ha^{-1} (22% of average yield) and 232 kg ha^{-1} (15% of average yield) for both methods, respectively. Dadhwal et al. (2003), simulating wheat growth based on leaf area index, found a RMSE value of 335 kg ha^{-1} in the sub-humid region of India. Also in this region, Mkhabela et al. (2011) using MODIS-NDVI reported a minimum RMSE value of 462 kg ha^{-1} and a bias value of 117 kg ha^{-1} in sub-humid zones of Canadian Prairies. Moriondo et al. (2007) found RMSE values of 440 and 470 kg ha^{-1} using AVHRR-NDVI data to predict wheat yield in Italy. In relation to forecasting yield, we obtained a proper prediction of wheat crop yield 1 month before harvest.

Table 4
Error statistics of satellite derived soybean and wheat yield estimates in the four analyzed agro-climatic zones.

Agro-climatic zones (crop)	RMSE (ka ha^{-1})[a]	Bias (kg ha^{-1})	*d*
Sandy Pampas (soybean)	376 (13)	216	0.88
Endorreic Pampas (soybean)	366 (12)	169	0.81
Northern hills (wheat)	556 (14)	99	0.97
Semi-arid Plains (wheat)	307 (22)	270	0.90

[a] Numbers in brackets are percentages of average yield.

The obtained results and the differences in regression models can be analyzed theoretically considering the relationship between soil moisture availability and evapotranspiration. Monteith and Unsworth (1990) established that evapotranspiration rate is determined, among other factors, by the fraction photosynthetic active radiation and the canopy resistance, which is related to soil moisture availability. In this regard, a drying process can be divided in two stages. Initially, plants control the width of their stomatal apertures in such a way that photosynthesis of CO_2 influx is maximized and transpiration is minimized (Farquhar and Sharkey, 1982). Then, with decreasing soil moisture availability the photosynthesis process is reduced. Although these changes are easily reversible, the increase in canopy resistance and transpiration reduction can be mainly monitored from satellite through increase in LST. In an advanced stage of the stress process, photosynthetic systems are structurally damaged (pigments and leaf structure). These changes are noticeable not only with LST but also with VI (Friedl et al., 1995). On the other hand, crop yield can be affected by water excess. In that condition the fraction photosynthetic active radiation is reduced due to the high cloud cover, consequently the photosynthesis decreases. Moreover, frequently soil water excess is associated with conditions of hypoxia and vegetation in bad health (fungus, bacteria). These changes are detectable mainly through decreases in EVI. Thereby, the combination of LST and EVI allows us to study the entire water-soil-crop system, evaluating the moisture availability and the effect in crop yield.

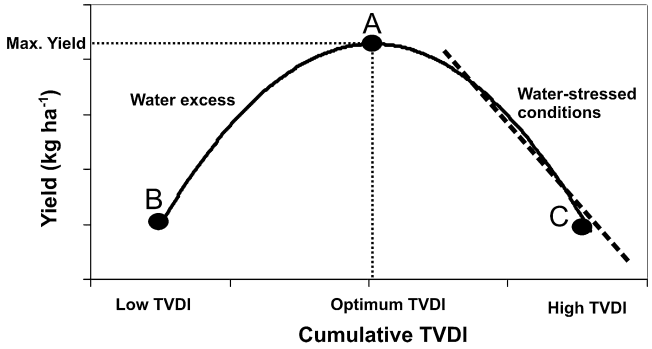

Fig. 8. Generalized model of crop yield and dryness index relationship. Maximum yield should be expected under normal water conditions (A) and minimum yield with water excess (BA line) and stress (AC line). Linear trend could be identifiable under predominant water stress conditions.

Based on these principles, the different obtained adjustments and the agro-climatic characteristics of the analyzed zones, a generalized model of the fluctuations of crop yield as a function of soil moisture availability is proposed (Fig. 8). This attempt to be the first comprehensive model derived from satellite data at regional scale. It should be noted that although the regression parameters should change this general model could be applicable in other regions of the world and crops. The model (Fig. 8) is best described by a quadratic function where a point of maximum yield (point A) can be defined, corresponding to intermediate values of TVDI and optimal soil moisture conditions (i.e. normal periods). Thus, there are no water limitations and the actual rate of photosynthesis is close to the photosynthetic capacity. Beyond this threshold, yield losses increase. Minimum crop yield should be expected under water excess (low TVDI, BA line) in poorly drained areas with long periods of waterlogging. On the other hand, decreasing yield should be observed with intensive water stress (high TVDI, AC line) in well drained areas or soils with low water retention capacity. Although the general model is described by a quadratic function, a linear trend (dotted line) could appear specifically in case of predominant water stress conditions (i.e. arid, semi-arid regions or crops with high water consumption).

6. Conclusions

The present study has shown that the TVDI method, which considers land surface temperature and vegetation index relationship, can be used effectively to derive soil moisture availability and predict crop yield one to three months before harvest over different agro-climatic zones of Argentine Pampas. Several possible error sources were considered and the traditional method of TVDI was improved using EVI instead of NDVI. Furthermore, as TVDI parameters are established empirically, the soil moisture estimates based on an image at one time cannot be compared with those at another date. A method based on dry and wet edges parameters is proposed to make them comparable.

First, this dryness index showed a strong correlation with soil moisture content measurements, with R^2 values ranged from 0.61 to 0.83 and also was in agreement with spatial pattern of soil moisture over the region, showing the suitability for spatial estimation of this variable at large scale. Then, the relationship with crop yield was successfully estimated. Depending on the agro-climatic zone, the models accounted for 68–79% and 76–81% of the yield variability of soybean and wheat, respectively. The RMSE approximate values were 366 and 380 kg ha^{-1} for soybean and for wheat they varied between 300 and 550 kg ha^{-1}, while the bias values ranged from 169 to 216 and 99 to 270 kg ha^{-1}, respectively. The overall errors of estimates were found to be comparable with the top validation results available worldwide for crop yield estimation using satellite data. In many cases, these results were better than others obtained with vegetation index (Basnyat et al., 2004; Mkhabela et al., 2005; Moriondo et al., 2007; Wall et al., 2008), showing the greater aptitude of surface temperature and vegetation index combination to reflect the crop water condition. Finally, the analysis of a wide range of soil moisture availability allowed us to develop a generalized model of crop yield in function of the dryness index that could be applicable in other regions and crops. In this context, several earlier studies have estimated near-surface soil moisture from satellite (Mallick et al., 2009; Sandholt et al., 2002; Wang et al., 2011, among others). However, frequently vegetation can extract soil water from the root zone. Future attempts should aim at evaluating the decoupling between near-surface and root zone soil moisture in vegetated pixels through LST/VI combination to improve crop yield estimation models.

It should be noted that, although the developed models imply progress in crop yield forecasting, they have limitations. The TVDI estimates potential yield, not taking into account what happens to the crop after the forecast date. Thus, diseases or drought could affect the vegetation while the models would most likely overestimate crop yield. However, these developments are valuable in areas where yield measurements are not available or with poor data coverage, as only satellite data are needed. In this sense, the use of satellite image products can provide a suitable tool for decision makers.

Acknowledgements

This work was carried out as a part of the project “Sustainable development and health care”, funded by the Agencia Nacional de Promoción Científica y Tecnológica of Argentina (ANPCyT). We are thankful to Ministerio de Agricultura, Ganadería y Pesca for providing part of used soil moisture measurements. Instituto de Hidrología de Llanuras and CONICET are all acknowledged for their contributions to this work.

Appendix A. Supplementary data

Supplementary data associated with this article can be found, in the online version, at http://dx.doi.org/10.1016/j.jag.2013.12.006. These data include Google maps of the most important areas described in this article.

References

Baez-Gonzalez, A.D., Chen, P., Tiscareno-Lopez, M., Srinivasan, R., 2002. Using satellite and field data with crop growth modelling to monitor and estimate corn yield in Mexico. Crop Sci. 42, 1943–1949.

Balaghi, R., Tychon, B., Eerens, H., Jlibene, M., 2008. Empirical regression model using NDVI, rainfall and temperature data for the early prediction of wheat grain yields in Morocco. Int. J. Appl. Earth Obs. Geoinf. 10, 438–452.

Basnyat, P., McConkey, B., Lafond, G.R., Moulin, A., Pelcat, Y., 2004. Optimal time for remote sensing to relate to crop grain yield on the Canadian prairies. Can. J. Plant Sci. 84, 97–103.

Batlivala, P.P., Ulaby, F.T., 1977. Feasibility of monitoring soil moisture using active microwave remote sensing. University of Kansas Center for Research, Inc., Remote Sensing Laboratory Technical Report No. 264-12.

Benedetti, R., Rossini, P., 1993. On the use of NDVI profiles as a tool for agricultural statistics: the case study of wheat yield estimate and forecasting in Emilio Romagna. Remote Sens. Environ. 45, 311–326.

Bhattacharya, B.K., Mallick, K., Nigam, R., Dakore, K., Shekh, A.M., 2011. Efficiency based wheat yield prediction in a semi-arid climate using surface energy budgeting with satellite observations. Agric. For. Meteorol. 151, 1394–1408.

Boulet, G., Chehbouni, A., Gentine, P., Duchemin, B., Ezzahar, J., Hadria, R., 2007. Monitoring water stress using series of observed to unstressed surface temperature difference. Agric. For. Meteorol. 146, 159–172.

Boken, V.K., Shaykewich, C.F., 2002. Improving an operational wheat yield model using phenological phase-based Normalized Difference Vegetation Index. Int. J. Remote Sens. 23, 4155–4168.

Brubaker, L., Entekhabi, D., 1996. Analysis of feedback mechanisms in land-atmosphere interaction. Water Resour. Res. 32, 1343–1357.
Capehart, W.J., Carlson, T.N., 1997. Decoupling of surface and near-surface soil water content: a remote sensing perspective. Water Resour. Res. 33 (6), 1383–1395.
Carlson, T.N., Gillies, R.R., Perry, E.M., 1994. A method to make use of thermal infrared temperature and NDVI measurements to infer surface soil water content and fractional vegetation cover. Remote Sens. Rev. 9, 161–173.
Carlson, T.N., Gillies, R.R., Schmugge, T.J., 1995. An interpretation of methodologies for indirect measurement of soil water content. Agric. For. Meteorol. 77, 191–205.
Carlson, T.N., Ripley, D.A., 1997. On the relation between NDVI, fractional vegetation cover, and leaf area index. Remote Sens. Environ. 62, 241–252.
Carmona, F., Rivas, R., Ocampo, D., Schirmbeck, J., Holzman, M., 2011. Sensores para la medición y validación de variables hidrológicas a escala local y regional a partir del balance de energía. Aqualac 3 (1), 26–36.
Chauhan, N.S., Miller, S., Ardanuy, P., 2003. Spaceborne soil moisture estimation at high resolution: a microwave optical/IR synergistic method. Int. J. Remote Sens. 24 (22), 4599–4622.
Chen, C-F., Son, N-T., Chang, L-Y., Chen, C-C., 2011. Monitoring of soil moisture variability in relation to rice cropping systems in the Vietnamese Mekong Delta using MODIS data. Appl. Geogr. 31, 463–475.
Crow, W.T., Ryu, D., Famiglietti, J.S., 2005. Upscaling of field-scale soil moisture measurements using distributed land surface modelling. Adv. Water Resour. 28, 1–14.
Dadhwal, V.K., Sehgal, V.K., Singh, R.P., Rajak, D.R., 2003. Wheat yield modeling using satellite remote sensing with weather data: recent Indian experience. Mausam 54 (1), 253–262.
Doraiswamy, P.C., Cook, P.W., 1995. Spring wheat yield assessment using NOAA AVHRR data. Can. J. Remote Sens. 21, 43–51.
Du, Y., Ulaby, F.T., Dobson, M.C., 2000. Sensivity to soil moisture by active and passive microwave sensors. IEEE Trans. Geosci. Remote Sens. 38 (1), 105–113.
Dubois, P.C., Zyl, J., Engman, T., 1995. Measuring soil moisture with imaging radars. IEEE Trans. Geosci. Remote Sens. 33 (4), 915–926.
Eagleman, J.R., Li, W.C., 1976. Remote sensing of soil moisture by a 21-cm passive radiometer. J. Geophys. Res. 81, 3660–3666.
Farquhar, G.D., Sharkey, T.D., 1982. Stomatal conductance and photosynthesis. Annu. Rev. Plant Physiol. 33, 317–345.
Friedl, M.A., Davis, F.W., 1994. Sources of variation in radiometric surface temperature over a tallgrass praire. Remote Sens. Environ. 48, 1–17.
Friedl, C.B., Randerson, J.T., Malmstrom, C.M., 1995. Global net primary production: Combining ecology and remote sensing. Remote Sens. Environ 51, 74–88.
Gillies, R.R., Carlson, T.N., 1995. Thermal remote sensing of surface soil water content with partial vegetation cover for incorporation into climate models. J. Appl. Meteorol. 34, 745–756.
Gillies, R.R., Carlson, T.N., Gui, J., Kustas, W.P., Humes, K.S., 1997. A verification of the 'triangle' method for obtaining surface soil water content and energy fluxes from remote measurements of the Normalized Difference Vegetation Index (NDVI) and surface radiant temperature. Int. J. Remote Sens. 18 (15), 3145–3166.
Goetz, S.J., 1997. Multisensor analysis of NDVI, surface temperature and biophysical variables at a mixed grassland site. Int. J. Remote Sens. 18 (1), 71–94.
Goward, S.N., Xue, Y., Czajkowski, K.P., 2002. Evaluating land surface moisture conditions from the remotely sensed temperature/vegetation index measurements: an exploration with the simplified simple biosphere model. Remote Sens. Environ. 79 (2–3), 225–242.
Grayson, R.B., Western, A.W., 1998. Towards areal estimation of soil water content from point measurement: time and space stability of mean response. J. Hydrol. 207, 68–82.
Han, Y., Wang, Y., Zhao, Y., 2010. Estimating soil moisture conditions of the Greater Changbai Mountains by land surface temperature and NDVI. IEEE Trans. Geosci. Remote Sens. 48 (6), 2509–2515.
Hochheim, K.P., Barber, D.G., 1998. Spring wheat yield estimation for Western Canada using NOAA NDVI data. Can. J. Remote Sens. 24, 17–27.
Holzapfel, C.B., Lafond, G.P., Brandt, S.A., Bullock, P.R., Irvine, R.B., Morrison, M.J., May, W.E., James, D.C., 2009. Estimating canola (*Brassica napus* L.) yield potential using an active optical sensor. Can. J. Plant Sci. 89, 1149–1160.
Holzman, M.E., Rivas, R.E., 2011. ENSO effects on hydric conditions of Pampa Region: a preliminary evaluation using LST and EVI. In: Annals of XV Simpósio Brasileiro de Sensoriamento Remoto, Curitiba, Brasil, pp. 2244–2249.
Holzman, M.E., Rivas, R., Piccolo, M.C., 2012. Utilización de imágenes de temperatura radiativa e índice de vegetación mejorado para el estudio de las condiciones hídricas en la región pampeana. Revista de Geología Aplicada a la Ingeniería 28, 25–33.
Huete, A., Didan, K., van Leeuwen, W., Miura, T., Glenn, E., 2011. Chapter 26 MODIS vegetation indices. In: Ramachandran, B., Justice, C.O., Abrams, M.J. (Eds.), Land Remote Sensing and Global Environmental Change. Springer, New York, pp. 579–602.
Huete, A.R., Liu, H.Q., 1994. An error and sensitivity analysis of the atmospheric and soil-correcting variants of the NDVI for the MODIS-EOS. IEEE Trans. Geosci. Remote Sens. 32 (4), 897–905.
Irmak, S., Haman, D.Z., Bastug, R., 2000. Determination of crop water stress index for irrigation timing and yield estimation of corn. Agron. J. 92, 1221–1227.
Jackson, R.D., 1982. Canopy temperature and crop water stress. Adv. Irrig. 1, 43–85.
Jackson, R.D., Reginato, R.J., Idso, S.B., 1977. Wheat canopy temperature: a practical tool for evaluating water requirements. Water Resour. Res. 13, 651–656.
Jackson, R.D., Reginato, R.J., Idso, S.B., 1981. Canopy temperature as a crop water stress indicator. Water Resour. Res. 17, 1133–1138.
Jackson, T.J., Schmugge, J., Engman, E.T., 1996. Remote sensing applications to hydrology: soil moisture. J. Hydrol. Sci. 41 (4), 517–529.
Jackson, T.J., Schmugge, T.J., Wang, J.R., 1982. Passive microwave sensing of soil moisture under vegetation canopies. Water Resour. Res. 18, 1137–1142.
Kaufman, Y.J., Tanré, D., 1992. Atmospherically resistant vegetation index (ARVI) for EOS-MODIS. IEEE Trans. Geosci. Remote Sens. 30, 261–270.
Kogan, F.N., 1994. Application of vegetation index and brightness temperature for drought detection. Adv. Space Res. 15 (11), 91–100.
Lambin, E.F., Ehrlich, D., 1995. Combining vegetation indices and surface temperature for land-cover mapping at broad spatial scales. Int. J. Remote Sens. 16 (3), 573–579.
Liu, H.Q., Huete, A.R., 1995. A feedback based modification of the NDVI to minimize canopy background and atmospheric noise. IEEE Trans. Geosci. Remote Sens. 33, 457–465.
Ma, B.L., Dwyer, L.M., Costa, C., Cober, E.R., Morrison, M.J., 2001. Early prediction of soybean yield from canopy reflectance measurements. Agron. J. 93, 1227–1234.
Mahey, R.K., Singh, R., Sidhu, S.S., Narang, R.S., Dadhwal, V.K., Parihar, J.S., 1993. Pre-harvest state-level wheat acreage estimation using IRS-IA LISS-I data in Punjab (India). Int. J. Remote Sens. 14, 1099–1106.
Mallick, K., Battacharya, B.K., Patel, N.K., 2009. Estimating volumetric surface moisture content for cropped soils using a soil wetness index based on surface temperature and NDVI. Agric. For. Meteorol. 149, 1327–1342.
Marti, J., Bort, J., Slafer, G.A., Araus, J.L., 2007. Can wheat yield be assessed by early measurement of normalised difference vegetation index? Ann. Appl. Biol. 150, 253–257.
Mkhabela, M.S., Bullock, P., Raj, S., Wang, S., Yang, Y., 2011. Crop yield forecasting on the Canadian Prairies using MODIS NDVI data. Agric. For. Meteorol. 151, 385–393.
Mkhabela, M.S., Mkhabela, M.S., 2000. Exploring the possibilities of using NOAA AVHRR data to forecast cotton yield in Swaziland. Uniswa J. Agric. 9, 13–21.
Mkhabela, M.S., Mkhabela, M.S., Mashinini, N.N., 2005. Early maize yield forecasting in the four agro-ecological regions of Swaziland using NDVI data from NOAA's-AVHRR. Agric. For. Meteorol 129, 1–9.
Monteith, J.L., 1981. Evaporation and surface temperature. Quart. J. Roy. Meteor. Soc. 107, 1–27.
Monteith, J.L., Unsworth, M.H., 1990. Principles of Environmental Physics, second ed. Butterworths, London.
Moran, M.S., Clarke, T.R., Inoue, Y., Vidal, A., 1994. Estimating crop water deficit using the relation between surface-air temperature and spectral vegetation index. Remote Sens. Environ. 49, 246–263.
Moran, M.S., 2004. Thermal infrared measurement as an indicator of planet ecosystem health. In: Quattrochi, D. (Ed.), Thermal Remote Sensing in Land Surface Processes. CRC-Taylor & Francis, pp. 257–282.
Moriondo, M., Maselli, F., Bindi, M., 2007. A simple model of regional wheat yield based on NDVI data. Eur. J. Agron. 26, 266–274.
Nemani, R., Pierce, L., Running, S., Goward, S., 1993. Developing satellite-derived estimates of surface moisture status. J. Appl. Meteorol. 32 (3), 548–557.
Nemani, R., Running, S.W., 1997. Land cover characterization using multi-temporal red, near-IR and thermal-IR data from NOAA/AVHRR. Ecol. Appl. 7 (1), 79–90.
O'Shaughnessy, S.A., Evett, S.R., Colaizzi, P.D., Howell, T.A., 2011. Using radiation termography and thermometry to evaluate crop water stress in soybean and cotton. Agric. Water Manage. 98, 1523–1535.
Patel, N.R., Anapashsha, R., Kumar, S., Saha, S.K., Dadwal, V.K., 2009. Assessing potential of MODIS derived temperature/vegetation condition index (TVDI) to infer soil moisture status. Int. J. Remote Sens. 30, 23–39.
Prasad, A.K., Chai, L., Singh, R.P., 2006. Crop yield estimation model for Iowa using remote sensing and surface parameters. Int. J. Appl. Earth Obs Geoinf. 8 (1), 26–33.
Price, J.C., 1990. Using spatial context in satellite data to infer regional scale evapotranspiration. IEEE Trans. Geosci. Remote Sens. 28, 940–948.
Quarmby, N.A., Milnes, M., Hindle, T.L., Silleos, N., 1993. The use of multi-temporal NDVI measurements from AVHRR data for crop yield estimation and prediction. Int. J. Remote Sens. 14, 199–210.
Rasmussen, M.S., 1992. Assessment of millet yields and production in northern Burkina Faso using integrated NDVI from AVHRR. Int. J. Remote Sens. 13, 3431–3442.
Rhee, J., Jungho, I., Carbone, G.L., 2010. Monitoring agricultural drought for arid and humid regions using multi-sensor remote sensing data. Remote Sens. Environ. 144, 2875–2887.
Sandholt, I., Rasmussen, K., Andersen, J., 2002. A simple interpretation of the surface temperature/vegetation index space for assessment of surface moisture status. Remote Sens. Environ. 79 (2-3), 213–224.
Stisen, S., Sandholt, I., Nöörgard, A., Fensholt, R., Jensen, K.H., 2008. Combining the method with thermal inertia to estimate regional evapotranspiration-applied to MSG-SEVIRI data in the Senegal River basin. Remote Sens. Environ. 112, 1242–1255.
Statistics Argentina, 2012. Agricultural Estimates Data, http://old.siia.gov.ar/index.php/series-por-tema/agricultura (accessed July 2012).
Shutko, A.M., 1982. Microwave radiometry of lands under natural and artificial moistening. IEEE Trans. Geosci. Remote Sens. 20 (1), 18–26.
Tang, R., Li, Z.-L., Tang, B., 2010. An application of the Ts-VI triangle method with enhanced edges determination for evapotranspiration estimation from MODIS data in arid and semi-arid regions: implementation and validation. Remote Sens. Environ. 114, 540–551.
UNDP (United Nations Development Programme), 2009. Caracterización de la producción agrícola en Argentina frente al cambio climático,

http://www.undp.org.ar/docs/prensa/brief-06-cambios.pdf (accessed August 2012).
Unganai, L.S., Kogan, F., 1998. Drought monitoring and corn yield estimation in Southern Africa from AVHRR data. Remote Sens. Environ. 63, 219–232.
Vicente-Serrano, S., Cuadrat-Prats, J.M., Romos, A., 2006. Early prediction of crop production using drought indices at different time-scales and remote sensing data: application in Ebro Valley (north-east Spain). Int. J. Remote Sens. 27, 511–518.
Viglizzo, E.F., Frank, F.C., 2006. Ecological interactions, feedbacks, thresholds and collapses in the Argentine Pampas in response to climate and farming during the last century. Quatern. Int. 158, 122–126.
Viglizzo, E.F., Roberto, Z.E., Lértora, F.A., López Gay, E., Bernardos, J., 1997. Climate and land-use change in field-crop ecosystems of Argentina. Agric. Ecosyst. Environ. 66, 61–70.
Wall, L., Larocque, D., Pierre-Majorique, L., 2008. The early explanatory power of NDVI yield modelling. Int. J. Remote Sens. 29, 2211–2225.
Wang, Q., Adiku, S., Tenhunen, J., Granier, A., 2005. On the relationship of NDVI with leaf area index in a deciduous forest site. Remote Sens. Environ. 94, 244–255.
Wang, W., Huang, D., Wang, X.-G., Liu, Y.-R., Zhou, F., 2011. Estimation of soil moisture using trapezoidal relationship between remotely sensed land surface temperature and vegetation index. Hydrol. Earth Syst. Sci. 15, 1699–1712.
Wang, K.C., Li, Z.Q., Cribb, M.M., 2006. Estimation of evaporative fraction from a combination of day and night land surface temperatures and NDVI: a new method to determine Priestley-Taylor parameter. Remote Sens. Environ. 102, 293–305.
Wang, C., Qi, S., Niu, Z., Wang, J., 2004. Evaluating soil moisture status in China using the temperature-vegetation dryness index (TVDI). Can. J. Remote Sens. 30 (5), 671–679.
Wang, L., Qu, J.J., 2009. Satellite remote sensing applications for surface soil moisture monitoring: a review. Front. Earth Sci. China 3 (2), 237–247.
Wang, X.W., Xie, H.J., Guan, H.D., Zhou, X.B., 2007. Different responses of MODIS derived NDVI to root-zone soil moisture in semi-arid and humid regions. J. Hydrol. 340 (1–2), 12–24.
Willmott, C.J., 1981. On the validation of models. Phys. Geog. 2, 184–194.